

Effects of remote sensing pixel resolution on modeled energy flux variability of croplands in Iowa

W.P. Kustas^{a,*}, F. Li^a, T.J. Jackson^a, J.H. Prueger^b, J.I. MacPherson^c, M. Wolde^c

^aUSDA-ARS Hydrology and Remote Sensing Laboratory, Building 007, BARC-West, Beltsville, MD 20705, USA

^bUSDA-ARS National Soil Tilth Laboratory, 2150 Pammel Drive, Ames, IA 50011, USA

^cInstitute for Aerospace Research, National Research Council of Canada, Ottawa, Ontario, Canada

Received 11 September 2003; received in revised form 17 December 2003; accepted 18 February 2004

Abstract

With increased availability of satellite data products used in mapping surface energy balance and evapotranspiration (ET), routine ET monitoring at large scales is becoming more feasible. Daily satellite coverage is available, but an essential model input, surface temperature, is at 1 km or greater pixel resolution. At such coarse spatial resolutions, the capability to monitor the impact of land cover change and disturbances on ET or to evaluate ET from different crop covers is severely hampered. The effect of sensor resolution on model output for an agricultural region in central Iowa is examined using Landsat data collected during the Soil Moisture Atmosphere Coupling Experiment (SMACEX). This study was conducted in concert with the Soil Moisture Experiment 2002 (SMEX02). Two images collected during a rapid growth period in soybean and corn crops are used with a two-source (soil + vegetation) energy balance model, which explicitly evaluates soil and vegetation contributions to the radiative temperature and to the net turbulent exchange/surface energy balance. The pixel resolution of the remote sensing inputs are varied from 60 m to 120, 240, and 960 m. Model output at high resolution are first validated with tower and aircraft-based flux measurements to assure reliability of model computations. Histograms of the flux distributions and resulting statistics at the different pixel resolutions are compared and contrasted. Results indicate that when the input resolution is on the order of 1000 m, variation in fluxes, particularly ET, between corn and soybean fields is not feasible. However, results also suggest that thermal sharpening techniques for estimating surface temperature at higher resolutions (~ 250 m) using the visible/near infrared waveband resolutions could provide enough spatial detail for discriminating ET from individual corn and soybean fields. Additional support for this nominal resolution requirement is deduced from a geostatistical analysis of the vegetation index and surface temperature images.

© 2004 Elsevier Inc. All rights reserved.

Keywords: Remote sensing; Energy flux variability; Iowa

1. Introduction

Remote sensing estimates of the surface energy balance, and evapotranspiration (ET) in particular, provide a means to assess, in a spatially distributed manner, crop conditions and end-of-season yields at large spatial scales (Moran et al., 1995; Moulin et al., 1998). Such spatial information would also be very useful to agronomists who frequently evaluate the effects of crop genotype and management practices in terms of the ratio of yield per a unit area to water use or ET to produce such a yield (Gregory et al., 2000), commonly called the crop's water use efficiency (WUE). To estimate WUE

over a landscape comprised of various crop types, genotypes, soil conditions, and management practices requires spatial information only feasible with remote sensing.

Remotely sensed surface temperature is used as the key boundary condition by most, if not all, remote-sensing-based energy balance models for estimating ET (Kustas & Norman, 1996). These data must be at high enough pixel resolution to discriminate individual fields, which in the Midwest are typically on the order of 10^0 ha or $10^2 \times 10^2$ m in dimension. This length scale is smaller than the pixel resolution of remotely sensed surface temperature data available from satellites routinely observing the land surface. These include the Geostationary Environmental Satellite (GOES) having 4-km resolution, the Advanced Very High Resolution Radiometer (AVHRR) having nominally 1.1-km resolution and the Moderate-Resolution Imaging Spectroradiometer (MODIS) having 1-km resolution. Thus,

* Corresponding author. Tel.: +1-301-504-8498; fax: +1-301-504-8931.

E-mail address: bkustas@hydrolab.arsusda.gov (W.P. Kustas).

in many circumstances, satellite pixels will be comprised of multiple crops and/or land use. This results not only in the inability to discriminate individual field conditions but also can cause significant errors in the pixel-average ET estimated by the model, especially when subpixel variability in cover, roughness, and moisture is significant (Kustas & Norman, 2000b; Moran et al., 1997).

Townshend & Justice (1988) show that for a wide variety of landscapes, pixel resolutions on the order of 10^2 m are required to monitor land use/land cover changes.

The Land Remote Sensing Satellite (Landsat) and the Advanced Space-borne Thermal Emission Reflectance Radiometer (ASTER) instrument on Terra provide remotely sensed surface temperature at pixel resolutions < 100 m, but routine application is hindered by the low frequency of repeated coverage (~ 16 days) and the fact that with cloud cover, monthly observations are likely. This severely limits the utility of these sensors in providing routine monitoring of ET.

Recently, an algorithm using the physical relationship between surface temperature and vegetation index (VI)–vegetation cover estimate to sharpen remotely sensed surface temperature imagery to the higher resolution of the visible and near-infrared wavelength bands has been developed and tested (Kustas et al., 2003a). With MODIS, which now can provide coverage twice a day from Terra and Aqua satellite platforms, the interband resolution difference is a factor of 4 having 250 m for VI bands vs. 1000 m for surface temperature. Hence, surface temperatures at 250-m resolution are more likely to provide the level of spatial detail necessary for evaluating fluxes of individual land cover types.

This paper will focus on computing surface fluxes with Landsat imagery collected over central Iowa at several different resolutions with the two-source energy balance model proposed by Norman et al. (1995). Output at the highest resolution is first validated using tower and aircraft-based flux data from the Soil Moisture Atmosphere Coupling Experiment (SMACEX) conducted in concert with the Soil Moisture Experiment 2002 (SMEX02) during June and July near Ames, IA.

The remotely sensed surface temperature data are degraded from 60-m resolution from Landsat 7 and 120 m from Landsat 5 to 240-m resolution, representing a thermally sharpened MODIS image as would be derived by a procedure described in Kustas et al. (2003a), and to 960 m, which is nominally the surface temperature resolution from MODIS and from AVHRR. The impact of using the coarser resolution input data on discriminating surface fluxes from individual field sites is investigated through an analysis of the frequency distributions (histograms) of the sensible and latent heat fluxes. In addition, higher moments of the flux distributions at the different resolutions are compared with that of a Gaussian distribution. Consistency in these findings is evaluated using a geostatistical analysis (i.e., semivariogram technique) of the vegetation index and surface

temperature images. The semivariogram provides a means to estimate the minimum resolution required for resolving discrete land cover types (Atkinson, 1997a, 1997b). It has also been used with surface temperature imagery to help interpret the impact of resolution on model output–flux observation agreement (Friedl, 1996).

Of particular interest is to see if fluxes from individual corn and soybean fields are distinguishable at ~ 250 -m resolution. This would indicate that ET estimation at finer resolutions may not be warranted to discriminate different land cover/crops. If true, MODIS data could be used with thermal sharpening techniques to provide a greater possibility for routine ET monitoring.

The focus of this paper differs from previous studies evaluating the effect of sensor resolution and/or aggregation techniques on remote sensing-based flux model output (e.g., Friedl, 1997; Kustas & Humes, 1996; Moran et al., 1997; Sellers et al., 1997; Su et al., 1999). At spatial resolutions that will encompass several cover types, errors in flux estimation can be significant (Kustas & Norman, 2000b; Moran et al., 1997). However, because there was virtually no difference in the area average fluxes for the two images computed by the model using the various input resolutions, errors in flux estimation due to the use of aggregated remotely sensed input variables is considered minor.

The Landsat 5 scene from June 23 and the Landsat 7 scene from July 1 analyzed by Li et al. (2004) will be used. Although only a week apart, this is a period of rapid growth for corn and soybean crops, which comprise nearly 95% of the cover type for this region. Li et al. found that at 960-m resolution, there is significant loss of information concerning field scale variability. The impact of this loss in surface variability on model-derived fluxes is investigated here and is the next logical step in understanding the role of sensor resolution on assessing effects of land cover change.

2. Model description

A detailed description of original model can be found in Norman et al. (1995) with recent modifications of some of the algorithms that expand its application to a wider range of environmental and vegetation canopy cover conditions (Kustas & Norman, 1999a, 1999b, 2000a, 2000b).

This two-source modeling approach evaluates the temperature contribution of the vegetated canopy layer and soil/substrate to the radiometric surface temperature observation, and the resulting turbulent heat flux contributions driven by surface–air temperature differences with aerodynamic resistance parameterizations from the vegetation and soil components. The modeling strategy follows the conceptual two-source framework proposed by Shuttleworth & Wallace (1985) for partially vegetated surfaces (see also Shuttleworth & Gurney, 1990).

In the model, the satellite derived radiometric surface temperature is considered a composite temperature of the soil and canopy and expressed as:

$$T_r(\phi) \approx [f_v(\phi)T_c^4 + (1 - f_v(\phi))T_s^4]^{1/4} \quad (1)$$

where T_r is the satellite-derived radiometric surface temperature, T_c is the canopy temperature, T_s is the soil temperature, and $f_v(\phi)$ is the fractional vegetation cover from radiometer with a view angle of ϕ . A relationship between the fractional vegetation cover and leaf area index (LAI) is required for estimating aerodynamic resistances and net radiation divergence through the canopy layers and is assumed to be exponential (Norman et al., 1995).

$$f_v = 1 - \exp(-0.5\text{LAI}) \quad (2)$$

Similar to the partitioning of the composite radiometric temperature, the surface energy balance of the canopy and soil are explicitly computed as

$$R_{ns} = H_s + \text{LE}_s + G \quad (3)$$

$$R_{nc} = H_c + \text{LE}_c \quad (4)$$

where R_{ns} is the net radiation at the soil surface and R_{nc} is the net radiation of the vegetated canopy layer, H_c is the canopy sensible heat flux, H_s is the soil surface sensible heat flux, LE_c is the canopy latent heat flux, LE_s is the soil latent heat flux, and G is soil heat flux.

By permitting the soil and vegetated canopy fluxes to interact with each other (see Fig. 11 in Norman et al., 1995), H_c and H_s can be expressed as: with

$$H_c = \rho C_p \frac{T_c - T_{ac}}{r_x} \quad (5)$$

and

$$H_s = \rho C_p \frac{T_s - T_{ac}}{r_s} \quad (6)$$

so that the total sensible heat flux $H = H_c + H_s$ is equal to

$$H = \rho C_p \frac{T_{ac} - T_a}{r_a} \quad (7)$$

where T_a is the surface layer air temperature, T_{ac} is the air temperature in the canopy air layer, r_x is the total boundary layer resistance of the complete canopy of leaves, r_s is the resistance to sensible heat exchange from the soil surface, and r_a is aerodynamic resistance. The original resistance formulations are described in Norman et al. (1995) with recent revisions described in Kustas & Norman (1999a, 1999b, 2000a, 2000b). Weighting of the heat flux contributions from the canopy and soil components is performed indirectly by the partitioning of the net radiation between

soil and canopy and via the impact on resistance values from the fractional amount and type of canopy cover (see Kustas & Norman, 1999a).

For the latent heat flux from the canopy, the Priestley–Taylor formula is used to initially estimate LE_c

$$\text{LE}_c = \alpha_{PT} f_g \frac{\Delta}{\Delta + \gamma} R_{nc} \quad (8)$$

where α_{PT} is Priestley–Taylor parameter, which is normally set to a nominal value ~ 1.3 , except under sparse canopy cover conditions where the value can be higher for well-watered crops (Kustas & Norman, 1999b), f_g is the fraction of green vegetation, Δ is the slope of the saturation vapor pressure vs. temperature curve and γ is the psychrometric constant ($\sim 0.066 \text{ kPa } ^\circ\text{C}^{-1}$). The α_{PT} or f_g parameter is adjustable to accommodate stressed vegetation conditions (see Kustas et al., 2004) and the Priestley–Taylor parameterization can be dropped in cases where nonphysical solutions are obtained, such as daytime condensation at the soil surface (i.e., $\text{LE}_s < 0$). For further details concerning model convergence, see Norman et al. (1995) and Kustas et al. (2004).

The latent heat flux from the soil surface is solved as a residual in the energy balance equation

$$\text{LE}_s = R_{ns} - G - H_s \quad (9)$$

with G estimated as a fraction of the net radiation at the soil surface:

$$G = c_g R_{ns} \quad (10)$$

where the value of $c_g \sim 0.3$. The value of c_g varies with soil type and moisture conditions as well as time, due to the phase shift between G and R_{ns} over a diurnal cycle (Santanello & Friedl, 2003). However, for the midmorning to midday period, the value of c_g can be assumed constant (Kustas & Daughtry, 1990; Santanello & Friedl, 2003).

3. Data/site description and field conditions

3.1. Site description

The SMACEX/SMEX02 field campaign was conducted between mid-June and mid-July (Kustas et al., 2003b). This experiment is an interdisciplinary investigation involving a diverse set of field measurements. Measurements of the coupled exchange of water, carbon and energy between soil, vegetation, and atmosphere covered scales from patch/field using tower measurements to landscape and regional using aircraft-based flux observations. In addition, vegetation data, atmospheric data, and satellite and aircraft-based remote sensing data from visible, thermal, and microwave band sensors were collected. For more details see the web site (<http://hydrolab.arsusda.gov/smex02>).

The SMACEX study site (WC) surrounded the Walnut Creek Watershed (centered at 41.96 N. Lat. 93.6 W. Long.) and contained extensive vegetation and soil moisture sampling for SMEX02 at over 30 field sites. A major part of SMACEX involved measurements of surface energy, water and carbon fluxes at 14 towers sites, as well as mean and turbulent atmospheric boundary layer (ABL) properties with aircraft, ground-based lidar, and balloon sounding observations (Kustas et al., 2003b).

With the WC study area being the primary focus of SMACEX, the 14 flux towers were distributed over the WC area to obtain representative areal sampling (see Fig. 1). The National Research Council of Canada Twin Otter atmospheric research aircraft flew transects over the WC study area designed to fly over several of the flux towers and to be used as a means of estimating WC-scale momentum, water, energy, and carbon fluxes (see Fig. 1).

In a typical growing season, nearly 95% of the WC area as well as the region is covered by row crops. Corn and soybean were the main crop varieties, with 50% in corn, 40–45% in soybean, and the remaining 5–10% in forage and grains. The climate is humid and the average annual rainfall is around 835 mm with one third of the rainfall typically occurring during May and June.

3.2. Field conditions

During the SMACEX/SMEX02 field campaign, there was rainfall before the start of the experiment and then a dry down period until July 4. However, only some areas of WC received rain from this event and several other localized storms. A more widespread rain event occurred on July 10 where over 60 mm was recorded by the rain gage network over the WC site with similar amounts measured over the region. This resulted in surface soil moisture (0–5-cm depth) decreasing from near field capacity ~ 25 –30% in mid-June to ~ 5 –10% before the rains, and then returning

to field capacity values, particularly after the rainfall event on July 10.

Over this period, the corn and soybeans crops grew rapidly. Observations near flux towers indicated canopy heights started at nominally 15 and 75 cm, for the soybean and corn, respectively, and reached heights of ~ 40 and 200 cm by mid-July. With such dramatic increases in vegetation height, there were also significant increases in vegetation biomass and leaf area index. Detailed vegetation sampling data were collected on a weekly basis for flux tower and soil moisture sampling sites within the WC study area (Anderson et al., 2004). Preliminary analyses indicate that leaf area index (LAI) sampling in mid-June gave LAI ~ 0.5 for soybean and ~ 1 for corn and by mid-July LAI sampling yielded values ranging ~ 1 to 3 and ~ 1.5 to 5 for soybean and corn, respectively. The large range in LAI values, particularly for corn, are due to microtopographic and soil textural variations across field sites as well as rainfall received during the field campaign (Anderson et al., 2004).

3.3. Satellite data

Two days of Landsat data were used for flux mapping at different pixel resolutions. The Landsat 5 overpass on June 23, 2002, viewed a partial canopy covered surface with LAI values from ground samples ~ 1 for soybeans and ~ 2 for corn. A significantly higher cover condition existed by the July 1, 2002, for the Landsat 7 overpass where ground samples indicated LAI ~ 2 for soybeans and 3.5 for corn. For details about how the Landsat data were processed to derive land surface temperature and NDVI, see Li et al. (2004). The technique to derive Normalized Difference Water Index (NDWI) is similar to that of NDVI, except that Landsat band 5 is used instead of band 3.

The two-source model requires two vegetation parameters for calculating the resistances. Nominal values are

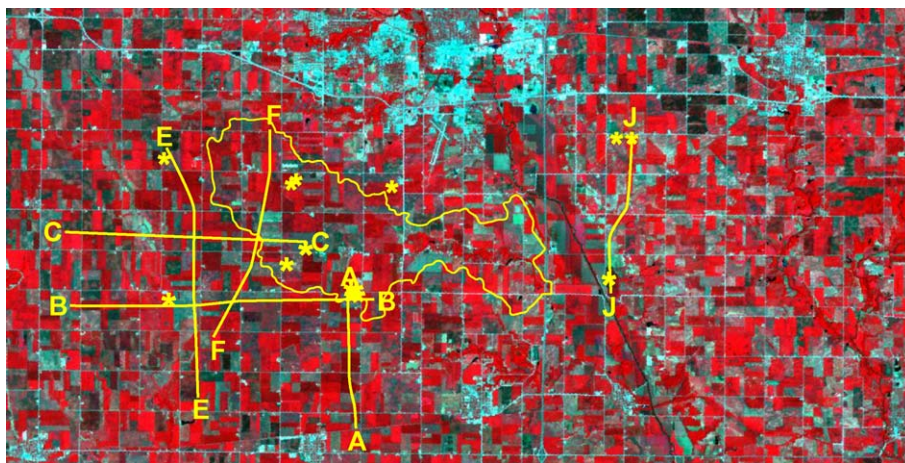


Fig. 1. A false-color Landsat 7 image from July 1, 2002, indicating the boundary of the WC study area and the Walnut Creek watershed. The star symbols denote approximate location of the flux towers and lines labeled by letters A, B, C, E, F, and J are the flight tracks of the Twin Otter.

needed because the model is not very sensitive to these values (Anderson et al., 1997; Zhan et al., 1996). The parameters include vegetation height and leaf width, both of which can be estimated from land classification. As part of SMEX02/SMACEX, a land cover database was developed at a 30-m spatial resolution using the Landsat data and is described in Jackson et al. (2004).

3.4. Flux measurements from towers and aircraft

During SMACEX/SMEX02, 14 eddy covariance flux stations were installed in the WC area. All flux stations had a Campbell Scientific (CSI) CSAT3 3-D sonic anemometer and 10 had a LiCor LI-7500 water vapor/ CO_2 sensor with the remaining 4 having a CSI Krypton Hygrometer (KH20).¹ Flux measurements were nominally 2 m above ground level (agl) over the soybean sites and 4 m agl over the corn sites. Half-hourly averaged turbulent fluxes (H and LE) were computed, while 10-min averages of net radiation and soil heat flux were stored. In addition, 10-min average ancillary meteorological data, such as air temperature, relative humidity, and wind speed were also recorded. Flux data from 12 of the 14 stations were collected in both “flux mode” where only the turbulent statistics of the raw 20-Hz data are recorded and in “time series” mode, which means all the raw 20-Hz data are retained not only for computing turbulent fluxes, but also for investigating turbulent properties.

The NRC Twin Otter aircraft measured fluxes and mean air properties approximately 40 m agl over six tracks ranging in length from 6 to 12 km (see Fig. 1). Most flights included at least two soundings, which provided atmospheric profiles from about 20 m above the surface to about 300 m above the top of the mixed layer. MacPherson and Wolde (2002) summarize the Twin Otter measurement campaign and provide detailed descriptions of the instrumentation, flight log and processing of the data raw collected at 32 Hz. Some preliminary results are discussed in MacPherson et al. (2003).

Although the surface moisture considerably dried out before the rains in early July, the flux tower measurements indicated latent heat and carbon fluxes generally increased while sensible heat flux decreased resulting in the Bowen ratio ($BR = H/LE$) decreasing from ~ 1 for both corn and soybean at the start of SMACEX to ~ 0.5 for soybean and to ~ 0.25 for corn before the rains near the end of the study period (Kustas et al., 2003b). A similar result was obtained with the aircraft-based flux observations. In addition, there was a significant reduction in soil heat flux as the canopy cover increased from $\sim 50\%$ to nearly 100% by the end of SMACEX. However, near the end of the dry down, there were visual signs of water stress at some field sites, which

contributed to the wide range in LAI values observed in mid-July (Anderson et al., 2004). This stressed condition was significant enough to have an impact at the WC scale because aircraft-based measurements showed a slight rise in the BR values before the rains.

3.5. Ground vegetation sampling

Vegetation data, such as vegetation height, leaf area index (LAI), and fractional vegetation cover were measured during the field experiment at 31 WC sites, which included field sites containing the flux towers. Each site was measured three to four times during the field experiment and contained three sampling areas representing low, high, and medium cover conditions. Relationships between vegetation indices using high-resolution aircraft and satellite data and LAI data were derived for scaling up the ground-based samples. Details of how the samples were taken and the resulting processing of the data is described by Anderson et al. (2004).

3.6. Model input data

The meteorological data, specifically wind speed and air temperature, used by the two-source model came from the 40-m observations from the Twin Otter. This measurement height was assumed to be within the “blending height” region (Wieringa, 1986) where the effects of surface heterogeneity are small and conditions are relatively uniform over a 5–10-km area. This height is typically on the order of 50 m above ground level (Raupach & Finnigan, 1995). Kustas et al. (1999) showed only a slight deterioration in the agreement between two-source heat flux estimation and measurements using mixed layer vs. local wind and air temperature observations. Incoming solar radiation was measured by the flux towers and was uniform during the satellite overpass.

The NDWI, land surface temperature, and land cover classification images were used as input data to obtain land surface flux images. The LAI, fractional vegetation cover, and crop height for each pixel were calculated from NDWI values. For mixed pixels at coarser resolutions containing different land-use/land cover, canopy height was computed as the weighted average of different vegetation types comprising the pixel. Surface roughness length and displacement height were then estimated as a function of canopy height and roughness lengths of the different land cover types comprising the mixed pixel as described by Shuttleworth et al. (1997).

Anderson et al. (2004) found that among a number of vegetation indices, NDWI derived from Landsat was least affected by saturation at high cover values. Hence, its relationship with LAI and crop height (h_c) based on ground LAI measurements showed the most stability and was therefore used to establish empirical relationships with LAI and h_c . The empirical modeling indicated that these relationships were nonlinear.

¹ Trade and company names are given for the benefit of the reader and imply no endorsement by the USDA.

4. Model results

4.1. Flux results—validation

The results from the two-source canopy model were used to compare with the tower and aircraft-based flux measurements. At the time of writing this paper, an error in the latent heat flux (and carbon flux) measurements was discovered by the manufacturer of the LI-7500 water vapor/CO₂ sensor. This error can be corrected, but requires reprocessing all the time series data and additional analyses to correct the data collected in “flux mode” (J.H. Prueger, personal communication). Therefore, only net radiation, sensible heat flux, and soil heat flux measurements were used directly. Latent heat fluxes were calculated as the residual in the surface energy balance, namely $LE = R_n - G - H$. Because the focus of this paper is not model validation, the comparisons between model and observations are only meant to provide the reader with reassurance that the model computes reliable fluxes.

The results listed in Table 1 indicate that the model estimated fluxes for an average of 2–4 pixels upwind of each tower are reasonably close to the measurements. The root mean square difference (RMSD) values are all under 45 $W m^{-2}$, which is within the uncertainty of surface flux measurements (Kustas & Norman, 2000b). The results for July 1 are slightly better with RMSD values less than 35 $W m^{-2}$. This is likely due to the thermal data resolution on July 1 being 60 m, which allows for better spatial sampling of the model output at scales commensurate with the flux tower source areas (Schuepp et al., 1990).

The aircraft-based flux measurements made within 30 min of the two Landsat overpasses are the average values for the whole aircraft transect. To compare with the flux observations, the model output was also averaged along the aircraft track as well as all pixels 2 km upwind, to consider the aircraft flux footprint (Schuepp et al., 1990). With winds from the south for both days and transect B flown closest during satellite overpass (see Fig. 1), model output for a rectangular box ~ 12 km east–west and ~ 2 km north–south was averaged. The comparison between model output and the aircraft-based measurements listed in Table 2

Table 1
Comparison between tower-based measurements and model flux estimates

		Tower ($W m^{-2}$)	Model ($W m^{-2}$)	RMSD ($W m^{-2}$)
June 23, 2002	Rn	593	572	29
	G	98	121	32
	H	91	71	26
	LE	404	381	43
July 1, 2002	Rn	619	609	23
	G	73	87	21
	H	111	101	25
	LE	435	420	34

Listed are average energy balance components from towers vs. model output and root mean square difference (RMSD) statistic.

Table 2
Comparison between aircraft-based measurements along Track B and model flux estimates

		Aircraft ($W m^{-2}$)	Model ($W m^{-2}$)	Diff ($W m^{-2}$)
June 23, 2002	Rn	581	563	18
	G	–	123	–
	H	112	90	12
	LE	329	350	21
July 1, 2002	Rn	627	602	25
	G	–	94	–
	H	126	121	5
	LE	332	388	56

Listed are average energy balance components from aircraft vs. model output and the absolute difference.

indicate differences in H of ~ 5 and 20 $W m^{-2}$ and for LE differences of ~ 20 and 55 $W m^{-2}$.

Because the model requires energy balance closure, namely $R_n - G = H + LE$, while the aircraft measurements do not, this is an additional source for disagreement between the model estimated and measured fluxes. To satisfy energy balance closure with flux measurements, Twine et al. (2000) suggests assuming that the value of BR from aircraft measurements is correct and use it in the energy balance equation to recalculate the sensible and latent heat fluxes. Assuming the average soil heat flux was 120 $W m^{-2}$ for June 23, and 100 $W m^{-2}$ for July 1 (average from the ground measurements) then the adjusted LE and H for the

Table 3
Mean, standard deviation and coefficient of variation of the energy balance components computed by the model at the different pixel resolutions

Date	Res. (number of pixels)	R_n	LE	H	G
<i>Mean ($W m^{-2}$)</i>					
June 23	120 m (46,512)	570	372	78	119
	240 m (11,552)	570	371	79	120
	960 m (703)	570	367	83	119
July 1	60 m (185,130)	603	391	118	94
	120 m (46,206)	603	392	117	94
	240 m (11,476)	603	393	116	94
	960 m (703)	604	391	119	94
<i>Standard deviation ($W m^{-2}$)</i>					
June 23	120 m (46,512)	18	65	33	19
	240 m (11,552)	17	61	31	17
	960 m (703)	11	40	21	11
July 1	60 m (185,130)	19	83	57	21
	120 m (46,206)	18	77	50	19
	240 m (11,476)	16	68	42	16
	960 m (703)	10	41	25	9
<i>Coefficient of variation (–)</i>					
June 23	120 m (46,512)	0.03	0.18	0.42	0.16
	240 m (11,552)	0.03	0.16	0.39	0.14
	960 m (703)	0.02	0.11	0.26	0.09
July 1	60 m (185,130)	0.03	0.21	0.49	0.22
	120 m (46,206)	0.03	0.20	0.43	0.20
	240 m (11,476)	0.03	0.17	0.36	0.17
	960 m (703)	0.02	0.10	0.21	0.09

aircraft measurements are 344 and 117 W m^{-2} for June 23 and 382 and 145 W m^{-2} for July 1, respectively. The “closed” aircraft-based fluxes significantly improve the agreement in LE while only slightly degrading the agreement in H .

The results in Tables 1 and 2 indicate that the model is in satisfactory agreement with both tower and aircraft-based flux measurements, suggesting that the model is computing reliable fluxes over the study area. Therefore, the results for the main phase of the study, an analysis of model output using different resolution remotely sensed input data, will have validity.

4.2. Flux results—pixel resolution

Anderson et al. (2004) demonstrated that the process of aggregating canopy conditions up to field scales was independent of the resolution of the remote sensing data used

provided that individual fields were resolved by the imagery. Hence, the variation between fractional canopy cover and vegetation indices that exist within a field is essentially linear. However, variability between fields was found to be nonlinear, thus pixel resolutions coarser than field scale will yield poor aggregate values unless subpixel information about cropping fractions is available. The fractional vegetation cover and surface temperature are key boundary conditions for the two-source model. Therefore, it is important to know how the pixel resolution of the remotely sensed input data affects model flux output. This is particularly the case for the operational satellites, which have thermal-infrared band pixel resolutions more coarse than the typical field dimensions in this region.

To address this issue, four different surface temperature–vegetation index resolutions are used with the two-source model for evaluating flux variability across the WC region. The pixel resolutions represent thermal-infrared band reso-

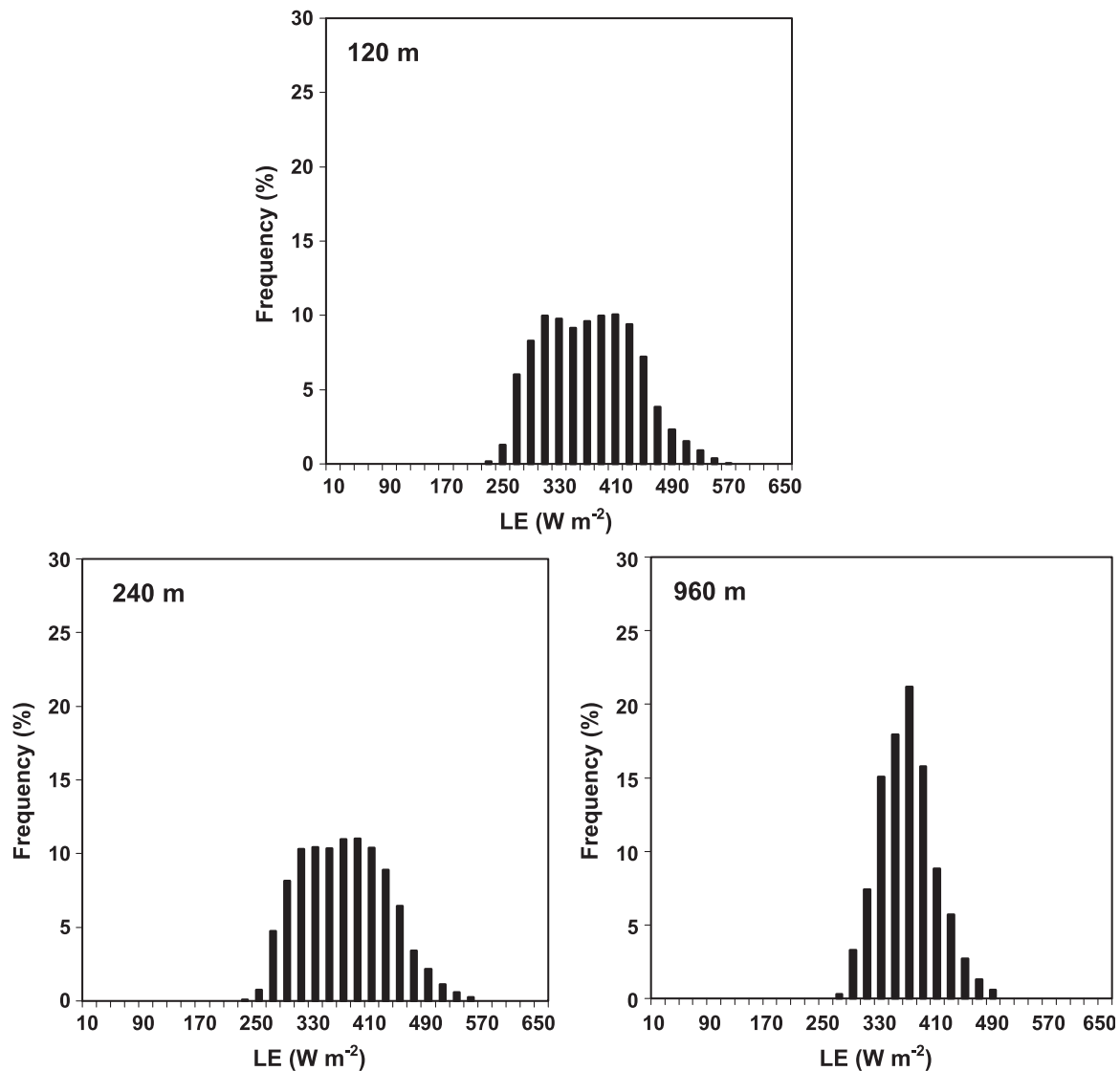


Fig. 2. Histograms for the LE distributions at the different resolutions for June 23, 2002, Landsat 5 overpass. Flux interval is 20 W m^{-2} .

lutions from Landsat 7 (60 m), Landsat 5 (120 m), a thermally sharpened surface temperature product (Kustas et al., 2003a) at the MODIS visible band (240 m) and the thermal-infrared band resolution from MODIS and AVHRR (960 m). The satellite-derived NDWI and T_r values were rescaled to the above resolutions and run with the two-source model for each different resolution. In addition, an experimental semivariogram (Atkinson, 1997a, 1997b; French, 2001) was computed using NDWI and T_r data to estimate a length scale representing the dominant landscape feature, which in this case would likely be the typical field size, and compare to the effects of resolution on model output.

In Table 3, some statistics are listed for the four-energy balance components over the WC domain at the different input resolutions. These include the mean, the standard deviation, and the coefficient of variation (CV = standard deviation/mean). At the different resolutions, the mean flux

values for the domain remain virtually the same and hence suggest minor errors incurred in the simple aggregation of the remote sensing inputs. As expected, there is a trend of decreasing variance with coarser resolution. However, other studies show that such a trend with coarser resolution remotely sensed input data does not occur (e.g., Su et al., 1999). Both the degree of variability of the land features and the model used to assess flux variability will have an effect on the resolution–spatial variability relationship (Friedl, 1997). The largest change is at 960 m, where in many cases the standard deviations and CV values are reduced by nearly 50% from their values using the highest resolution data. This reduced variation in model output is particularly evident in the turbulent fluxes, H , and LE.

The variation in H and LE fluxes at the different resolutions was investigated in more detail. Histograms of the H and LE distributions were plotted and the normalized third and fourth moments, or the skewness and kurtosis, of

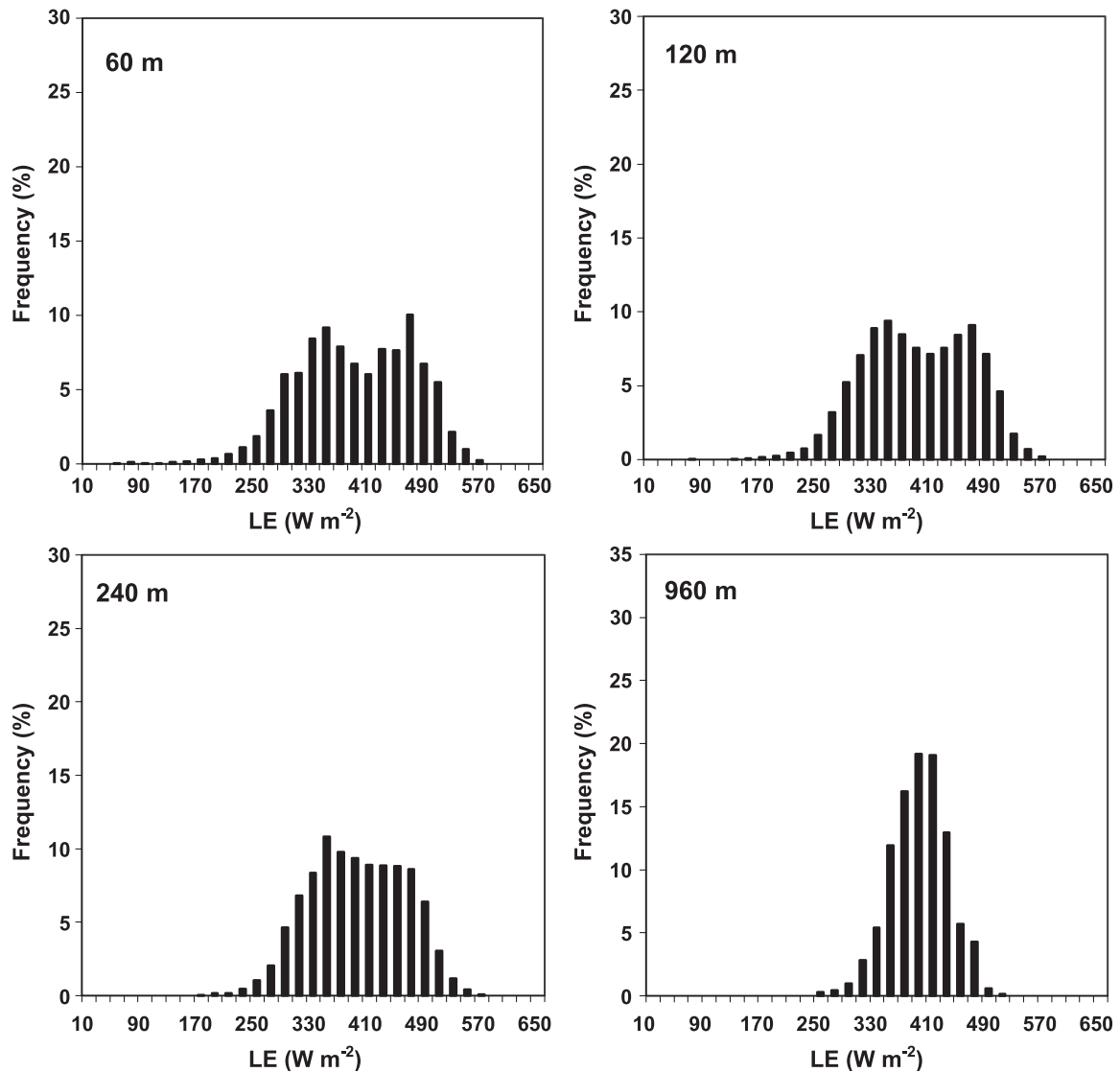


Fig. 3. Histograms for the LE distributions at the different resolutions for July 1, 2002, Landsat 7 overpass. Flux interval is 20 W m^{-2} .

Table 4
Skewness and kurtosis values for LE and H at the different pixel resolutions

Date	Res. (number of pixels)	LE		H	
		Skewness	Kurtosis	Skewness	Kurtosis
June 23	120 m (46,512)	0.22	2.34	-0.42	2.82
	240 m (11,552)	0.24	2.43	-0.45	2.83
	960 m (703)	0.35	3.11	-0.53	3.39
July 1	60 m (185,130)	-0.30	2.76	0.98	5.43
	120 m (46,206)	-0.17	2.46	0.65	4.29
	240 m (11,476)	-0.07	2.37	0.28	3.15
	960 m (703)	-0.23	3.11	0.50	4.23

the distribution were evaluated, providing a measure of the deviation from Normal (Gaussian). A normally distributed variable has skewness=0 and a kurtosis or flatness=3. The magnitude of the standard deviations for H and LE in Table 3 suggests 20 W m^{-2} is a reasonable value to be used as the flux interval for generating the histograms.

The histograms for the LE distributions at the different resolutions are illustrated for June 23 (Fig. 2) and July 1 (Fig. 3). The most dramatic change in histogram shape and distribution occurs in going from $\sim 10^2$ to 10^3 m pixel resolution, particularly for the July 1 case. A more dramatic change in LE distribution with resolution for July 1 is due not only to the higher resolution surface temperature data available from Landsat 7, but also the average difference in soybean and corn LE was higher on July 1 ($\sim 135 \text{ W m}^{-2}$) compared to June 23 ($\sim 100 \text{ W m}^{-2}$).

For July 1 at the 60-m resolution, two peaks in LE are evident at around $340\text{--}360 \text{ W m}^{-2}$ and the other at $460\text{--}480 \text{ W m}^{-2}$ (Fig. 3). These two peaks primarily come from soybean and corn fields, respectively. By July 1, the corn was reaching maturity, with LAI values generally between 2 and 4 while the soybean fields were still under partial canopy cover with LAI values between 0.5 and 2 (Anderson et al., 2004). These two peaks still exist when the resolution

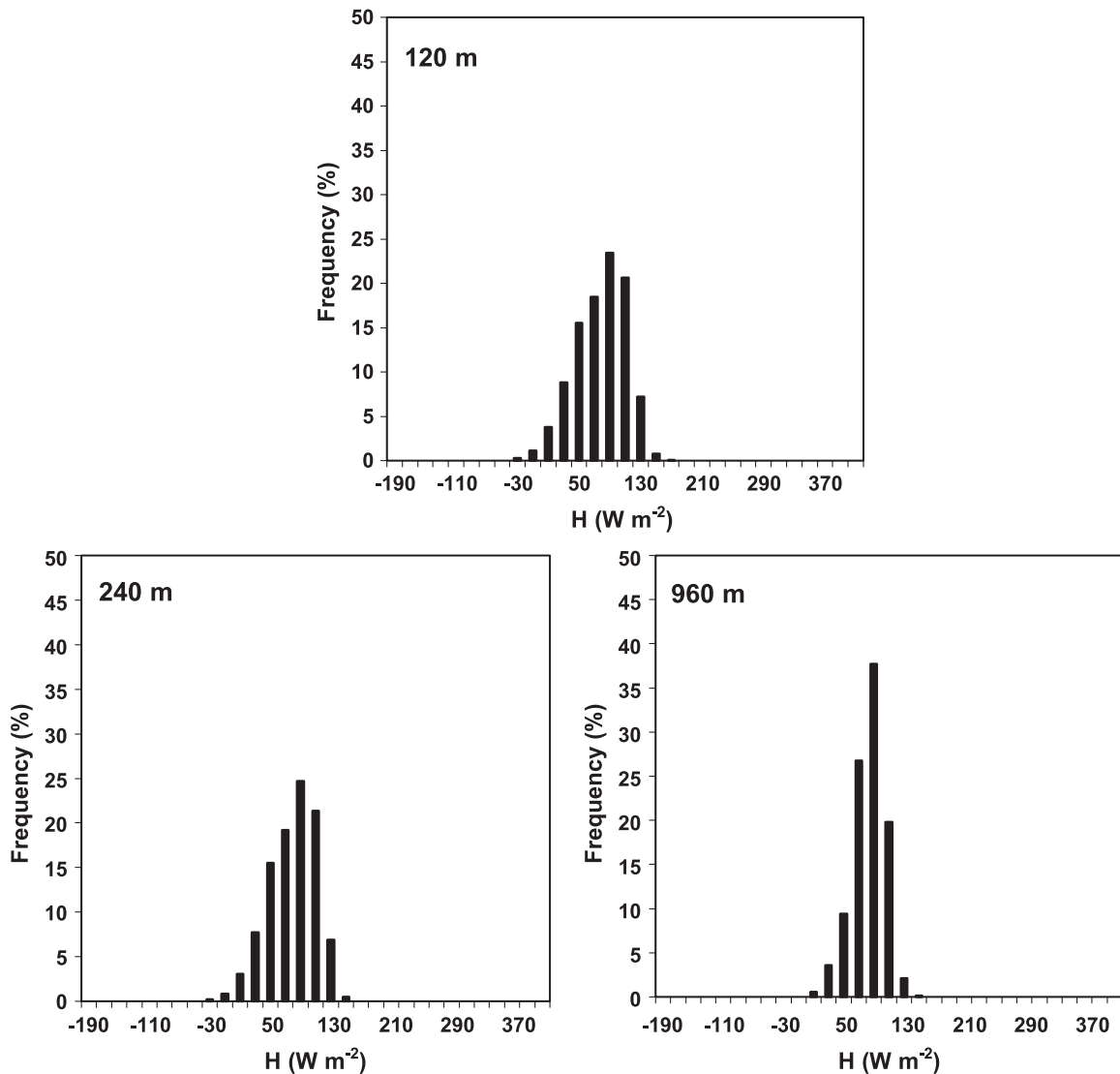


Fig. 4. Histograms for the H distributions at the different resolutions for June 23, 2002, Landsat 5 overpass. Flux interval is 20 W m^{-2} .

is degraded to 120 m but is more difficult to discern at 240-m resolution. At the 960-m resolution, any distinction between LE from corn and soybean crops is lost with approximately 80% of the LE values falling between 340 and 440 $W m^{-2}$.

For the June 23 image, the LE distribution at 120-m resolution contains two peaks, similar to July 1, but it is not as obvious (Fig. 2) and not very apparent even at the 240-m resolution. At the 960-m resolution, most LE values fall between 300 and 420 $W m^{-2}$, consistent with the July 1 case, but shifted to smaller values. In both June 23 and July 1 case, the shape of the LE distributions remains the same until the pixel resolution approaches 1000 m. This is also supported by the statistical results in Tables 3 and 4 (see below).

In Table 4, values of the kurtosis indicate the LE distributions for both June 23 and July 1 images are flatter than normal at the 10^2 -m resolutions and are close to a normal distribution by 960 m. The skewness values for all

resolutions are close to Gaussian or symmetrical about the mean, having either slightly positive (June 23) or negative (July 1) values. In general, as resolution is degraded, the LE distributions tend to be more normally distributed.

Histograms for the H distributions do not change as dramatically with the spatial resolution as LE (Figs. 4 and 5), nor are two peaks in H as apparent for the high resolution July 1 case, and virtually nonexistent for June 23. Although the standard deviations for H at the different resolutions are lower than for LE, the CV values are larger, indicating more variation compared to the average (Table 2). The kurtosis values listed in Table 4 indicate H is close to normally distributed for the June 23 output and has a slightly narrower distribution for the July 1 case, while the skewness values indicate the distributions are slightly asymmetrical with small negative (June 23) and positive (July 1) values. Thus the skewness and kurtosis of the H distributions change little with resolution.

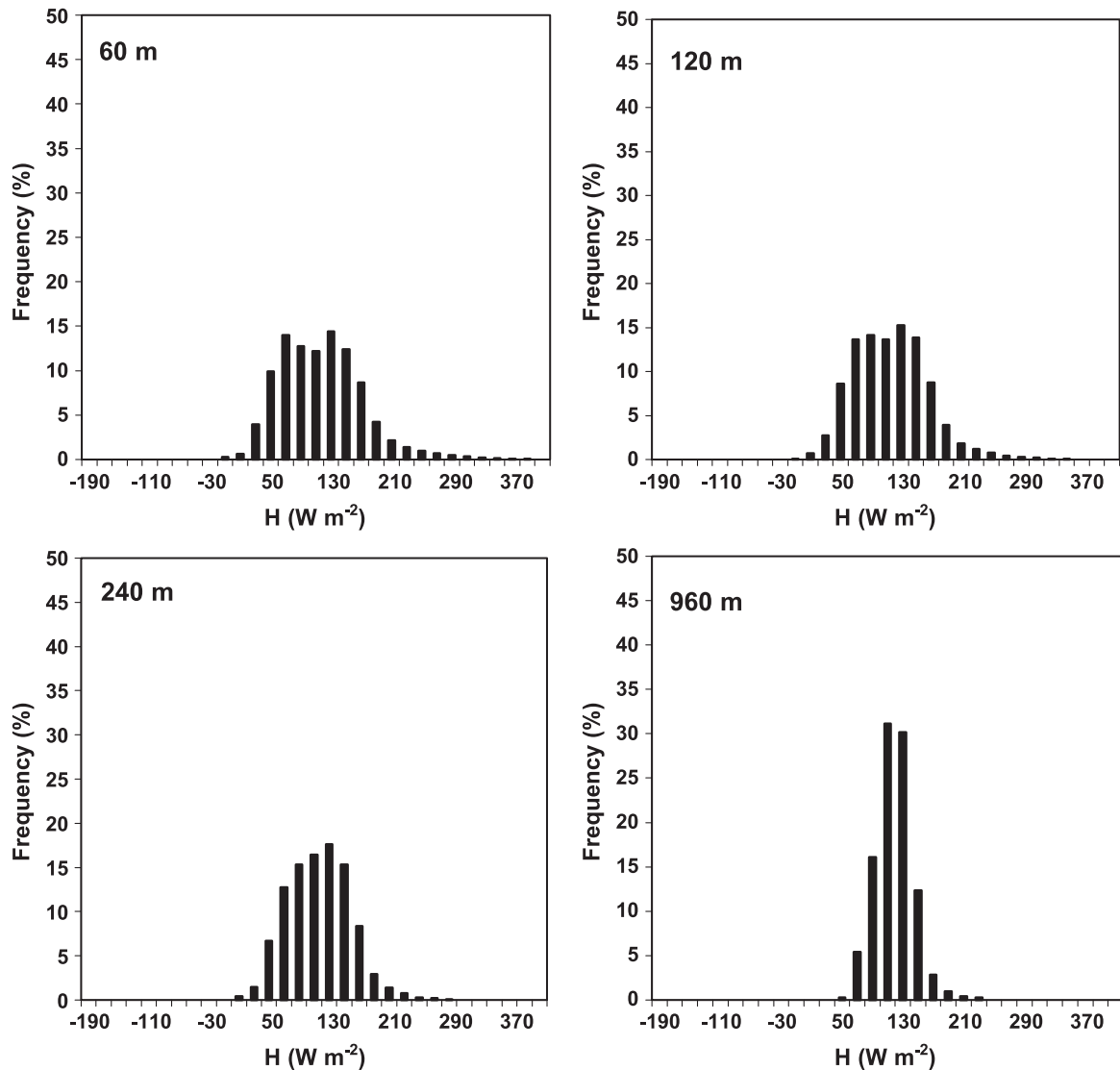


Fig. 5. Histograms for the H distributions at the different resolutions for July 1, 2002, Landsat 7 overpass. Flux interval is 20 $W m^{-2}$.

The results of the semivariogram analysis with NDWI for both days are illustrated in Fig. 6 and for T_r in Fig. 7. For the June 23 and July 1 imagery, the resolution of NDWI is 30 m, while the T_r data is four times coarser at 120 m for June 23 and twice as coarse at 60 m for July 1. For NDWI, the threshold semivariance value or sill indicative of the lag distance or range where the NDWI pixels are relatively uncorrelated is on the order of 500 m, with virtually no change in semivariance by ~ 800 m for both days (Fig. 6). These lag distances help to define length scales of the dominant landscape/land cover feature (as defined by NDWI), beyond which coarser resolution imagery will be comprised of mixture of these land surface features. For T_r , the sill is reached at a slightly greater lag distance of ~ 600 – 800 m for both days (Fig. 7). However, with T_r having coarser pixel resolution, determining the sill and range is more difficult especially for the June 23 imagery.

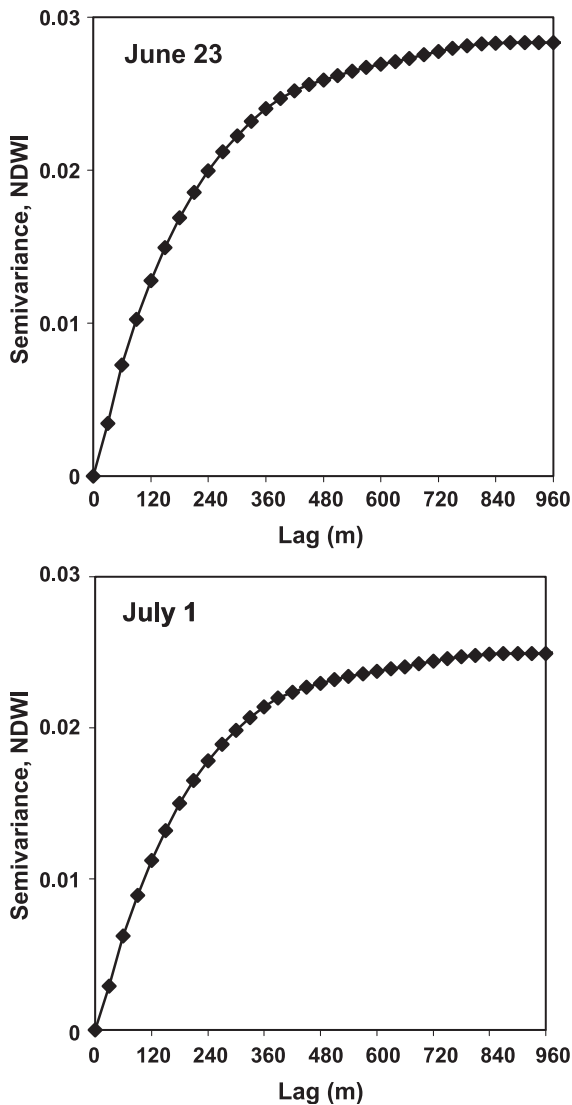


Fig. 6. Experimental semivariogram of NDWI from June 23 Landsat 5 and July 1 Landsat 7 imagery.

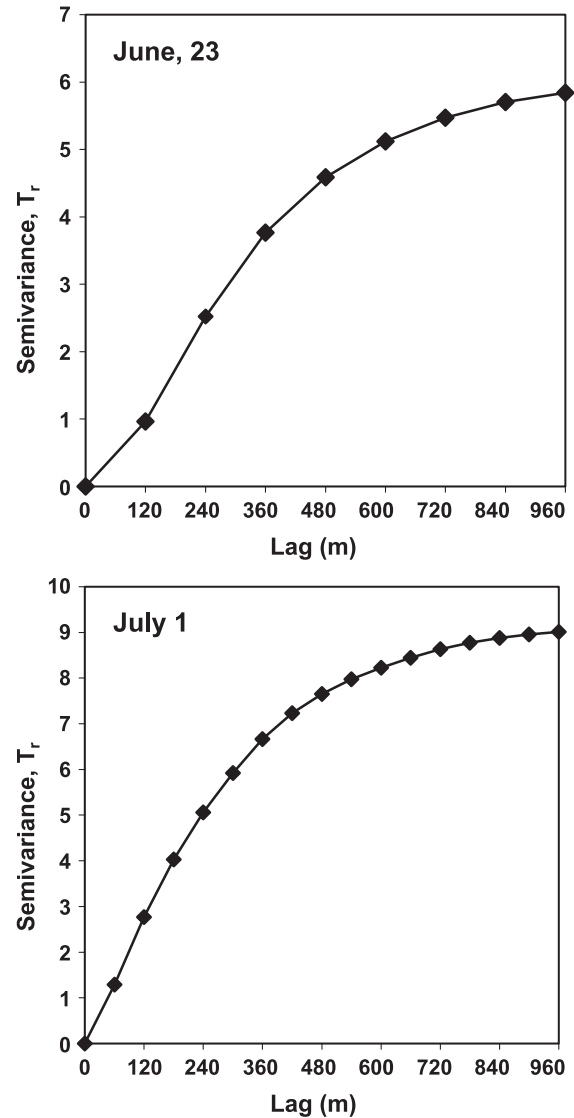


Fig. 7. Experimental semivariogram of T_r from June 23 Landsat 5 and July 1 Landsat 7 overpass.

Both of these results indicate that a pixel resolution of less than 500 m is recommended to sample individual fields and discriminate between crop types.

5. Summary and conclusions

The two-source model was applied to Landsat 5 and 7 imagery collected over central Iowa during the SMEX02/SMACEX study. Model flux estimates were shown to be in reasonable agreement with tower-based and aircraft-based flux measurements providing confidence in model output. Changing the pixel resolution of the remote sensing inputs to the model indicates that a dramatic change in the spatial distribution of the fluxes, particularly LE, occurs at the 960-m pixel resolution. At this resolution, information pertaining to individual corn and soybean fields is lost with model

input comprised of a mixture of both crops. At 240-m resolution, the two LE peaks from primarily the soybean and corn crops evident at the higher resolutions (especially at 60 m from the July 1 Landsat 7 overpass) are more difficult to define. However, the LE distributions and statistical properties at 240-m resolution are still similar to the higher resolution output. Consistent with these results is the semivariogram analysis performed with NDWI and the T_r data. The geostatistical results for the key remotely sensed inputs to the model indicate that the minimum resolution to resolve discrete land surface types should be less than ~ 500 m.

This analysis suggests that using MODIS thermal-infrared band resolution of 1000 m will be too coarse over this region for distinguishing LE variations between corn and soybean fields. Moreover, any associated model inputs at this coarse resolution will represent a mixture of corn and soybean crops, which will cause errors in the application of crop-specific relations using the remote sensing data (Atkinson, 1997a). Errors in flux model output at the coarser resolutions will depend on the magnitude and areal extent of the contrast in surface conditions within a model grid or remote sensing pixel (Kustas & Norman, 2000b). Consequently, studies using actual remote sensing imagery have given mixed results indicating minor errors (e.g., Friedl, 1997; Sellers et al., 1995) as well as significant errors (Moran et al., 1997; Su et al., 1999) can occur in flux computations with coarser resolution inputs.

The results of this study as well as previous investigations on aggregation/resolution effects suggest that the use of thermal sharpening techniques such as the one described in Kustas et al. (2003a) should be applied where possible to gain information on subpixel variability. For MODIS, this sharpening technique permits the thermal-infrared sensor data to be downscaled to the 250 m visible and near-infrared band resolution for assessing vegetation cover conditions. At this higher resolution, the results indicate that a significant amount of the spatial information would be retrievable (for this agricultural region), and LE from individual corn and soybean fields could still be evaluated. This could then provide for more routine monitoring of crop water use and condition, ultimately providing a way to evaluate water use efficiency and yield potential from different crops and management practices in a spatially distributed manner.

Acknowledgements

Funding provided by NASA grant S-44825-G under NRA 00-OES-07 from the NASA Terrestrial Hydrology Program made possible the SMACEX project. Logistical support from the USDA-ARS National Soil Tilth Lab and the SMEX02 project were critical in the success of the SMACEX field campaign.

References

- Anderson, M. C., Norman, J. M., Diak, G. R., Kustas, W. P., & Mecikalski, J. R. (1997). A two-source time-integrated model for estimating surface fluxes using thermal infrared remote sensing. *Remote Sens. Environ.*, *60*, 195–216.
- Anderson, M. C., Neale, C. M., Li, F., Norman, J. M., Kustas, W. P., Jayanthi, H., & Chavez, J. (2004). Upscaling ground observations of vegetation cover and water content during SMEX02 using aircraft and landsat imagery. *Remote Sensing of Environment*, *92*, 475–482 (this issue).
- Atkinson, P. M. (1997a). Selecting the spatial resolution of airborne MSS imagery for small-scale agricultural mapping. *International Journal of Remote Sensing*, *18*(9), 1903–1917.
- Atkinson, P. M. (1997b). On estimating error in remotely sensed images with the variogram. *International Journal of Remote Sensing*, *18*(14), 3075–3084.
- French, A.N., (2001). Scaling of surface energy fluxes using remotely sensed data. PhD thesis, University of Maryland, 336 pp.
- Friedl, M. A. (1996). Relationships among remotely sensed data, surface energy balance, and area-averaged fluxes over partially vegetated land surfaces. *Journal of Applied Meteorology*, *35*, 2091–2103.
- Friedl, M. A. (1997). Examining the effects of sensor resolution and subpixel heterogeneity on spectral vegetation indices: Implications for biophysical modeling. In D. A. Quattrochi, & M. F. Goodchild (Eds.), *Scale in Remote Sensing and GIS* (pp. 113–139). New York: CRC Lewis Publishers.
- Gregory, P. J., Simmonds, L. P., & Pilbeam, C. J. (2000). Soil type, climatic regime, and the response of water use efficiency to crop management. *Agronomy Journal*, *92*, 814–820.
- Jackson, T. J., Chen, D., Cosh, M. H., Li, F., Walthall, C., Anderson, M., & Doraiswamy, P. (2004). Vegetation water content mapping using Landsat TM derived NDWI for corn and soybean. *Remote Sensing of Environment* (in press).
- Kustas, W. P., & Daughtry, C. S. T. (1990). Estimation of the soil heat flux/net radiation ratio from spectral data. *Agricultural and Forest Meteorology*, *49*, 205–223.
- Kustas, W. P., & Humes, K. S. (1996). Variations in the surface energy balance for a semi-arid rangeland using remotely sensed data at different spatial resolutions. In J. B. Stewart, E. T. R. Engman, A. Feddes, & Y. Kerr (Eds.), *Scaling up in Hydrology using Remote Sensing* (pp. 127–145). London: Wiley. Chap. 8.
- Kustas, W. P., & Norman, J. M. (1996). Use of remote sensing for evapotranspiration monitoring over land surfaces. *Hydrological Science Journal*, *41*, 495–516.
- Kustas, W. P., & Norman, J. M. (1999a). Reply to comments about the basic equations of dual-source vegetation–atmosphere transfer models. *Agricultural and Forest Meteorology*, *94*, 275–278.
- Kustas, W. P., & Norman, J. M. (1999b). Evaluation of soil and vegetation heat flux predictions using a simple two-source model with radiometric temperature for partial canopy cover. *Agricultural and Forest Meteorology*, *94*, 13–29.
- Kustas, W. P., & Norman, J. M. (2000a). A two-source energy balance approach using directional radiometric temperature observations for sparse canopy covered surface. *Agronomy Journal*, *92*, 847–854.
- Kustas, W. P., & Norman, J. M. (2000b). Evaluating the effects of subpixel heterogeneity on pixel average fluxes. *Remote Sensing of Environment*, *74*, 327–342.
- Kustas, W. P., Prueger, J. H., Humes, K. S., & Starks, P. J. (1999). Estimation of surface fluxes at field scale using surface layer versus mixed-layer atmospheric variables with radiometric temperature observation. *Journal of Applied Meteorology*, *38*, 224A–238A.
- Kustas, W. P., Norman, J. M., Anderson, M. C., & French, A. N. (2003a). Estimating subpixel surface temperatures and energy fluxes from the vegetation index–radiometric temperature relationship. *Remote Sensing of Environment*, *85*, 429–440.
- Kustas, W. P., Jackson, T. J., Prueger, J. H., Hatfield, J. L., & Anderson, M. C.

- (2003b). Remote sensing field experiments for evaluating soil moisture retrieval algorithms and modeling land-atmosphere dynamics in central Iowa. *EOS Transactions of the American Geophysical Union*, 84(45), 485–493.
- Kustas, W. P., Norman, J. M., Schmugge, T. J., & Anderson, M. C. (2004). Mapping surface energy fluxes with radiometric temperature. (Chapter 7) In: D. A. Quattrochi, & J. C. Luvalle (Eds.), *Thermal Remote Sensing in Land Surface Processes* (pp. 205–253). Boca Raton, Florida: CRC Press.
- Li, F., Jackson, T. J., Kustas, W. P., Schmugge, T. J., French, A. N., Cosh, M., & Bindlish, R. (2004). Deriving land surface temperature from Landsat 5 and 7 during SMEX02/SMACEX. *Remote Sensing of Environment*, 92, 521–534 (In this issue).
- Macpherson, I., Mengistu, W., Kustas, W., & Prueger, J. (2003). Aircraft and tower-based measured fluxes over rapidly growing corn and soybean crops in Central Iowa during SMACEX. Proceedings of the Hydrology Conference, American Meteorological Society Annual Meeting, Feb. 9–13, 2003, Long Beach, CA. Preprint CD-ROM.
- MacPherson, J. L., Wolde, M., (2002). NRC Twin Otter operations in the soil moisture–atmosphere coupling experiment (SMACEX). Laboratory Technical Report. LTR-FR-190, National Research Council of Canada, Ottawa, 26 pp.
- Moran, M. S., Humes, K. S., & Pinter Jr., P. J. (1997). The scaling characteristics of remotely-sensed variables for sparsely-vegetated heterogeneous landscapes. *Journal of Hydrology*, 190, 337–362.
- Moran, M. S., Maas, S. J., & Pinter Jr., P. J. (1995). Combining remote sensing and modeling for estimating surface evaporation and biomass production. *Remote Sensing Reviews*, 12, 335–353.
- Moulin, S., Bondeau, A., & Delécolle, R. (1998). Combining agricultural crop models and satellite observations: From field to regional scales. *International Journal of Remote Sensing*, 19, 1021–1036.
- Norman, J. M., Kustas, W. P., & Humes, K. S. (1995). A two-source approach for estimating soil and vegetation energy fluxes in observations of directional radiometric surface temperature. *Agricultural and Forest Meteorology*, 77, 263–293.
- Raupach, M. R., & Finnigan, J. J. (1995). Scale issues in boundary-layer meteorology: Surface energy balance in heterogeneous terrain. *Hydrological Processes*, 9, 589–612.
- Santanello, J. A., & Friedl, M. A. (2003). Diurnal covariation in soil heat flux and net radiation. *Journal of Applied Meteorology*, 42, 851–862.
- Schuepp, P. H., Leclerc, M. Y., MacPherson, J. I., & Desjardins, R. L. (1990). Footprint prediction of scalar fluxes from analytical solutions of the diffusion equation. *Boundary-Layer Meteorology*, 50, 355–373.
- Sellers, P. J., Heiser, M. D., Hall, F. G., Verma, S. B., Desjardins, R. L., Schuepp, P. M., & MacPherson, J. I. (1997). The impact of using area-averaged land surface properties—topography, vegetation condition, soil wetness—in calculations of intermediate scale (approximately 10 km²) surface–atmosphere heat and moisture fluxes. *Journal of Hydrology*, 190, 269–301.
- Sellers, P. J., Heiser, M.D., Hall, F. G., Goetz, S. J., Strebel, D. E., Verma, S. B., Desjardins, R. L., Schuepp, P. M., & MacPherson, J. I. (1995). Effects of spatial variability in topography, vegetation cover and soil moisture on area-averaged surface fluxes: A case study using FIFE 1989 data. *J. Geophys. Res.*, 100(D12), 25607–25629.
- Shuttleworth, W. J., & Gurney, R. J. (1990). The theoretical relationship between foliage temperature and canopy resistance in sparse crops. *Quarterly Journal of the Royal Meteorological Society*, 116, 497–519.
- Shuttleworth, W. J., & Wallace, J. S. (1985). Evaporation from sparse crops—an energy combination theory. *Quarterly Journal of the Royal Meteorological Society*, 111, 839–855.
- Shuttleworth, W. J., Yang, Z.-L., & Arain, M. A. (1997). Aggregation rules for surface parameters in global models. *Hydrology and Earth System Sciences*, 2, 217–226.
- Su, Z., Pelgrum, H., & Menenti, M. (1999). Aggregation effects of surface heterogeneity in land surface processes. *Hydrology and Earth System Sciences*, 3(4), 549–563.
- Townshend, J. G. R., & Justice, C. O. (1988). Selecting the spatial resolution of satellite sensors required for global monitoring of land transformations. *International Journal of Remote Sensing*, 9, 187–236.
- Twine, T. E., Kustas, W. P., Norman, J. M., Cook, D. R., Houser, P. R., Meyers, T. P., Prueger, J. H., Starks, P. J., & Wesely, M. L. (2000). Correcting eddy–covariance flux underestimates over a grassland. *Agriculture and Forest Meteorology*, 103, 279–300.
- Wieringa, J. (1986). Roughness-dependent geographical interpolation of surface wind speed averages. *Quarterly Journal of the Royal Meteorological Society*, 112, 867–889.
- Zhan, X., Kustas, W. P., & Humes, K. S. (1996). An intercomparison study on models of sensible heat flux over partial canopy surfaces with remotely sensed surface temperature. *Remote Sensing of Environment*, 58, 242–256.